

编号: 2024-1167

检索报告

受南通市第一人民医院张毅的委托,对其所提交的学术论文被收录和引用情况在 Web of Science(Science Citation Index Expanded)中进行了检索,以下 1 篇论文被 SCIE 收录。

第 1 条,共 1 条

标题: PGK1 Is Involved in the HIF-1 Signaling Pathway as a Hub Gene for Ferroptosis After Traumatic Brain Injury

作者: Wang, Z (Wang, Zhao); Tian, JJ (Tian, Jinjie); Wang, L (Wang, Lei); Yan, HY (Yan, Hongyan); Feng, SJ (Feng, Sujuan); **Zhang, Y (Zhang, Yi)**

来源出版物: MOLECULAR NEUROBIOLOGY DOI: 10.1007/s12035-024-04170-z Early Access Date: JUN 2024 Published Date: 2024 JUN 4

Web of Science 核心合集中的 "被引频次": 0

入藏号: WOS:001239296400002

文献类型: Article; Early Access

地址: [Wang, Zhao; Tian, Jinjie; Yan, Hongyan; Feng, Sujuan; Zhang, Yi] Nantong Univ, Dept Neurosurg, Affiliated Hosp 2, Nantong 226001, Peoples R China.

[Wang, Lei] Nantong Univ, Dept Emergency Ctr, Affiliated Hosp 2, Nantong 226001, Jiangsu, Peoples R China.

通讯作者地址: Feng, SJ; **Zhang, Y (通讯作者)**, Nantong Univ, Dept Neurosurg, Affiliated Hosp 2, Nantong 226001, Peoples R China.

电子邮件地址: takeucifsj@163.com; zhangyi9285@sina.com

ISSN: 0893-7648

eISSN: 1559-1182

期刊影响因子 (2022): 5.1

中科院 2023 年期刊大类分区 (升级版): 2 区

特此证明!





PGK1 Is Involved in the HIF-1 Signaling Pathway as a Hub Gene for Ferroptosis After Traumatic Brain Injury

Zhao Wang¹ · Jinjie Tian¹ · Lei Wang² · Hongyan Yan¹ · Sujuan Feng¹ · Yi Zhang¹

Received: 18 October 2022 / Accepted: 3 April 2024

© The Author(s), under exclusive licence to Springer Science+Business Media, LLC, part of Springer Nature 2024

Abstract

The pathogenesis of ferroptosis in traumatic brain injury (TBI) is unclear; therefore, we aimed to identify key molecules associated with ferroptosis in TBI using bioinformatics analysis to determine its underlying mechanisms. GSE128543 dataset was downloaded from the Gene Expression Omnibus (GEO) database, and TBI-associated modules were obtained by weighted gene co-expression network analysis (WGCNA). We identified 60 differentially expressed genes (DEGs) by intersecting the modules with ferroptosis and glycolysis/gluconeogenesis gene libraries. The hypoxia-inducible factor-1 (HIF-1) signaling pathway was identified to be critical for ferroptosis post-TBI, and protein–protein interaction (PPI) network identified 20 hub genes, including phosphoglycerate kinase 1 (*PGK1*), ribosomal protein (*RP*) family, pyruvate kinase M1/2 (*PKM*), hypoxia-inducible factor 1 α subunit (*HIF-1 α*), and *MYC* genes. In this study, we further explored the role of *PGK1*, a gene involved in HIF-1 signaling pathway; however, its role and mechanism in TBI are still unclear. Moreover, we constructed a TBI mouse model and examined *PGK1* and *HIF-1 α* expression levels, and the results revealed their expressions increased after cortical injury in mice and they co-localized in the same cells. Furthermore, we examined the expressions of *PGK1* in the cerebrospinal fluid of 20 clinical patients with different degrees of brain injuries within 48 h of surgery and examined the cognitive function of patients according to the Glasgow Coma Scale (GCS). The results revealed that *PGK1* expression level was negatively correlated with the severity of the brain injury. These findings suggest that *PGK1* may become a potential hub gene for ferroptosis via the HIF-1 signaling pathway, second to neurological injury after TBI, thereby affecting patient prognosis.

Keywords Traumatic brain injury · Ferroptotic genes · *PGK1* · HIF-1 signaling pathway · Bioinformatics

Introduction

Traumatic brain injury (TBI) has increased with the acceleration of urban construction and its associated increase in traffic accidents, and has led to a large consumption of social resources [1], with a 20% mortality rate and 50% incidence of

poor prognosis [2]. The post-traumatic phase following TBI leads to neurological, behavioral, and cognitive impairments that typically develop over a period of months to years after the trauma and significantly affect the quality of life [3, 4]. Craniocerebral injury includes two pathological stages: primary and secondary damage. The primary injury involves irreversible brain damage, vascular damage, and diffuse axonal injury, whereas the secondary injury is due to hypoxia, release of inflammatory mediators, and abnormal function of coagulation fibrinolysis and monocyte infiltration [5]. Brain tissue hypoxia promotes glycolytic and gluconeogenic processes [6], causing a decrease in glucose concentration and decrease in lactate concentration in patients with acute TBI [7, 8]. Ferroptosis is a newly discovered programmed cell death-like process that has been identified post-brain injury; however, its mechanism in TBI is unclear.

Ferroptosis is distinct from the traditional causes of cell death, such as apoptosis, necrosis, thermal hypoplasia, and autophagy [9]. It was first reported in 2012 and has

Zhao Wang, Yi Zhang and Jinjie Tian contributed equally to this work and share first authorship.

✉ Sujuan Feng
takeucifsj@163.com

✉ Yi Zhang
zhangyi9285@sina.com

¹ Department of Neurosurgery, The Second Affiliated Hospital of Nantong University, Nantong 226001, China

² Department of Emergency Center, The Second Affiliated Hospital of Nantong University, Nantong 226001, Jiangsu, China

been associated with the progression of several diseases, including tumors, stroke, kidney injury, and hematological damage, primarily due to its pathology of accumulation of iron-dependent oxidants, which is characterized by iron-dependent lipid peroxidation [10–15]. Recent studies have suggested that ferroptosis is associated with brain injury-related cell death mechanisms, and a study using HT22 neuronal cells and C57BL/6 TBI-mouse model suggested that ferroptosis may be involved in the pathogenesis of TBI in vitro and in vivo [16]. It was found that the expression levels of some hub molecules, particularly, the hypoxia-inducible factor 1 α subunit (HIF-1 α) involved in the ferroptosis induction process, were altered after ferroptosis [17, 18]. Currently, bioinformatics-based studies on ferroptosis genes post-brain injury are limited. Therefore, in this study, we used data mining and weighted gene co-expression network analysis (WGCNA) techniques to screen for differentially expressed genes (DEGs) in cortical and normal brain tissues of TBI mice. We identified 60 differentially expressed genes (DEGs) by intersecting the modules with ferroptosis and glycolysis/gluconeogenesis gene libraries. The hypoxia-inducible factor-1 (HIF-1) signaling pathway was identified to be critical for ferroptosis post-TBI, and protein–protein interaction (PPI) network identified 20 hub genes, including phosphoglycerate kinase 1 (*PGK1*), ribosomal protein (*RP*) family, pyruvate kinase M1/2 (*PKM*), hypoxia-inducible factor 1 α subunit (*HIF-1 α*), and *MYC* genes. As there are numerous RP family molecules involved, we have not focused on them in this study and have chosen to target *PGK1*, which is involved in the HIF-1 signaling pathway, while we expect that other molecules may be validated in subsequent work. *PGK1* was selected for further analysis and its hub transcription factors (TFs), miRNAs, and interventional drugs were predicted. Additionally, a mouse TBI model was constructed to test the above hypothesis.

PGK1 is a hub enzyme in anaerobic and aerobic glycolysis. During glycolysis, *PGK1* catalyzes the transfer of phosphate group from 1,3-diphosphoglycerate (1,3-BPGA) to ADP to produce 3-phosphoglycerate (3-PGA) and an ATP, a high energy molecule. During gluconeogenesis, *PGK1* catalyzes the reverse reaction and forms 1,3-BPGA and ADP [19, 20]. Since the forward reaction is one of the two ATP-producing steps in the glycolytic pathway, it is important in the metabolism of many organisms, and studies have confirmed its role in tumor development [21]. Furthermore, *PGK1* expression is increased in rat TBI tissues [22]. Additionally, studies have demonstrated that HIF-1 α upregulates a series of glycolytic genes during glycolysis and uses *PGK1* as a downstream target and that glycolysis is necessary to maintain HIF-1 α activity [23]. Another study demonstrated that *PGK1* increases HIF-1 α activity [24]. Moreover, HIF-1 α is involved in regulating the process of secondary brain injury after TBI and has shown to play an important

role in several central nervous system diseases [25]. HIF-1 α is a major transcriptional regulator of the hypoxic response and facilitates the regulation of cell survival under various stresses. A recent study showed that HIF-1 pathway activation after upregulation of HIF-1 α has an inhibitory effect on ferroptosis [26]; however, at present, the role of *PGK1* in the ferroptosis is unclear.

Our results will help to understand the impact of ferroptosis process on secondary brain injury post-TBI, provide new ideas for clinical diagnosis and treatment of brain injury, and provide more insight on the mechanism of *PGK1* in secondary neurological injury post-TBI and in the development and prognosis of TBI. This project may provide theoretical support for the elucidation of the mechanisms of secondary injury due to ferroptosis post-TBI and may provide a therapeutic strategy for improving the prognosis of TBI patients, having far-reaching clinical significance.

Materials and Methods

Data Acquisition

The dataset GSE128543, containing data on differential gene expression changes in cerebral cortex tissue of controlled cortical impact injury induced TBI mice model, was downloaded from the Gene Expression Omnibus (GEO) database (<https://www.ncbi.nlm.nih.gov/geo>). Additionally, cortical tissue samples from seven TBI mice and seven controls were included in the analysis. Ferroptosis and glycolysis/gluconeogenesis datasets were obtained from the GeneCards database for the management and identification of ferroptosis-related markers and regulators.

WGCNA

WGCNA was used to search for modules with co-expressed genes and explore the relationship between these modules and hub genes associated with the phenotypes. Using gene expression profiles, we calculated the median absolute deviation (MAD) of each gene and eliminated the top 50% of the genes with the smallest MAD and the outlier genes and samples using the *goodSamplesGenes* method of the R package WGCNA. We further used WGCNA to construct scale-free co-expression network. At first, Pearson's correlation matrices and average linkage method were both performed for all the pair-wise genes. Thereafter, a weighted adjacency matrix was constructed using a power function: $A_{mn} = |C_{mn}|^\beta$ (C_{mn} is the Pearson's correlation between gene m and gene n ; A_{mn} is the adjacency between gene m and gene n). β was a soft-thresholding parameter that could emphasize strong correlations between genes and penalize weak correlations. After setting β as 4, the adjacency was transformed into a

topological overlap matrix (TOM), which could measure the network connectivity of a gene, defined as the sum of its adjacency with all the other genes for network generation, and the corresponding dissimilarity (1-TOM) was calculated. To classify genes with similar expression profiles into gene modules, average linkage hierarchical clustering was conducted according to the TOM-based dissimilarity measure with a minimum size (gene group) of 30 for the gene dendrogram. To further analyze the module, we calculated the dissimilarity of module eigengenes, chose a cut line for module dendrogram, and merged some modules. In addition, we merged modules with <0.25 distances and obtained 22 co-expression modules. Notably, the grey module was considered as the set of genes that could not be assigned to any module.

Functional Enrichment Analysis

Functional enrichment analysis was performed using gene ontology (GO) and Kyoto encyclopedia of genes and genomes (KEGG) databases. GO database contains three domains, including biological process (BP), cellular component (CC), and molecular function (MF), while the KEGG database contains datasets of pathways involving biological functions, diseases, chemicals, and drugs. The enrichment analysis was carried out by using clusterProfiler R package to determine the biological functions of the genes and associated pathways. The gene sets were restricted to a minimum of 5 and a maximum of 5000. *P*-value of <0.05 and a FDR of <0.25 were considered statistically significant.

Protein–Protein Interaction (PPI) Network Analysis

Search Tool for the Retrieval of Interacting Genes/Proteins (STRING), an online database which can retrieve the interaction between a group of proteins, was used to predict PPIs. Cytoscape network visualization was obtained with interaction scores >0.4 . The nodes represented genes and the edges represented the links between the genes. In addition, the PPI network was built and visualized using Cytoscape v3.6.0 software.

Gene-miRNA/Drug Interaction Networks

NetworkAnalyst (<https://www.networkanalyst.ca/NetworkAnalyst>) was used to predict drugs, TFs, and miRNAs targeting the marker genes. The literature-curated regulatory interaction data was collected from the RegNetwork repository to predict targeted pivotal TF-miRNA co-regulatory interactions and construct the interaction networks. We also used DrugBank database (v5.0) to predict the drugs.

TBI Model

Male C57BL/6 mice (8–12 weeks old) were provided by the Laboratory Animal Center of Nantong University. Animal experiments, which were in accordance with the National Institutes of Health (NIH) Guide for the Care and Use of Laboratory Animals, were approved by the Animal Experimentation Committee of Nantong University. The brain stereotaxic instrument (Hubei Medical Bioinstrumentation Co., Ltd.), anti-HIF-1 α antibody (20,960–1-AP, USA), anti-PGK1 antibody (17,811–1-AP, USA), and anti-glyceraldehyde-3-phosphate dehydrogenase (GAPDH) antibody (60,004–10-Ig, USA) were purchased from Proteintech; anti-glial fibrillary acidic protein (anti-GFAP) antibody (G3893, USA) was purchased from Sigma-Aldrich; anti-neuronal nuclear protein (anti-NeuN) antibody (66,836–1-Ig, USA) was purchased from Proteintech; and anti-ionic calcium binding protein (Iba) antibody (019–19741, Japan) was purchased from Wako. In this experiment, the mouse brain injury model was prepared by the cortical stab injury method, as follows: mice were weighed and anesthetized intraperitoneally with 10% chloral hydrate solution (0.3 mL/100 g), and the surgical area (middle of the head) was shaved and wiped with iodine and alcohol. The scalp was incised along the middle of the head, approximately 2 cm to the right, and the skull was exposed by bluntly separating the soft tissues and the epicranial membrane. A circular bone window of 4-mm diameter was opened with a cranial drill, 2 mm in front of the herringbone suture and 2 mm to the midline of the skull, keeping the dura intact. The skull was inserted sagittally into the right cerebral cortex with a scalpel to a depth of 2 mm. The mice were killed within 1–7-day post-injury and morphological and biochemical analyses were performed as described below. In the sham-operated group, the cranial window was opened and then closed with bone wax, and no cut was applied. The observation time points after model establishment were set as sham, 3-h, 1-day, 3-day, and 7-day post-TBI for specimen collection.

Modified Neurological Severity Score (mNSS)

mNSS was used to assess neurological function in each group. The scoring scale included motor function tests (muscle status and abnormal activity), sensory function tests (visual, tactile, and proprioceptive), physiological reflex tests, and balance tests, which were used to assess long-term neurological function. Each group of six mice was scored at 3-h, 1-day, 3-day, and 7-day post-TBI. The scale scores ranged from 0 (normal score) to 18 (maximum deficit score), and a score of 1 was assigned if the mice were unable to perform the test or did not respond as expected (Supplementary Table 1).

Wet and Dry Method for Measuring Cerebral Edema

The wet and dry weight method was used to determine the water content of the brain tissue. After preparing the mouse TBI model, the ischemic brain tissue was removed and its wet weight was measured immediately. Thereafter, the tissue was dried in a hot air oven at 105 °C for 48 h and its dry weight was measured. The water content in the brain tissue was calculated using the following formula:

$$\text{brain water content (\%)} = \frac{(\text{wet weight} - \text{dry weight})}{\text{wet weight}} \times 100$$

Hematoxylin–Eosin (HE) Staining

Five groups of six mice were fixed by perfusion with 4% paraformaldehyde, and the brains were removed, dehydrated, and then the frozen cortical Sects. (10-μm thick) were cut using a cryostat. Thereafter, the sections were subjected to the following treatments: anhydrous ethanol for 5 min, 90% ethanol for 2 min, 80% ethanol for 2 min, 70% ethanol for 2 min, distilled water for 2 min, hematoxylin staining solution for 10 min, tap water to wash off excess staining solution, differentiation solution for 30 s, tap water to rinse for 10 min, eosin staining solution for 1 min, 70% ethanol for 10 s, 80% ethanol for 10 s, and 90% ethanol for 10 s, 90% ethanol for 10 s, anhydrous ethanol for 10 s, and xylene for 5 min. Finally, the sections were sealed with neutral gum for microscopic observation.

Immunofluorescence Assay

After perfusion with 4% paraformaldehyde, mouse brains were removed, dehydrated, and the frozen cortical Sects. (10-μm thick) were cut using a cryostat. Subsequently, goat serum blocking solution was added dropwise for 1.5 h. Thereafter, PGK1 (1:100), GFAP (1:200), ionized calcium-binding protein (Iba1; 1:200), and NeuN (1:200) were added dropwise at 4 °C overnight. The sections were then incubated with secondary antibodies for 1.5 h in the dark. Lastly, the sections were incubated with diamidino diaminodiphenylindole (DAPI) stain for 5 min in the dark and the films were sealed and photographed.

Western Blot (WB)

After the mice were anesthetized and executed, the injured cortical tissues were obtained and incubated in tissue lysis solution. Thereafter, the sample was centrifugation at 12,000 rpm for 15 min, the supernatant was collected, and the total protein concentration was determined using the bicinchoninic acid (BCA) kit. Equal amounts of proteins

were transferred to polyvinylidene fluoride (PVDF, Merck Millipore) after sodium dodecyl sulfate–polyacrylamide gel electrophoresis (SDS-PAGE), and incubated at 4 °C with 5% skimmed milk for 2 h and overnight with primary antibodies: PGK1, HIF-1α (1:1000), and GAPDH (1:5000). The membrane was washed three times with tris-buffered saline Tween 20 (TBST), incubated with HRP-labeled secondary antibody for 2 h at room temperature, washed three times with TBST, and developed using the developing solution. Image J software was used for grayscale analysis, and GAPDH was used as the internal reference. The expression level of the target protein was indicated as the ratio of the grayscale value of the target protein to the grayscale value of GAPDH.

Analysis of Cerebrospinal Fluid (CSF) and Prognosis in Patients with TBI

Twenty emergency surgical patients (aged 18–85 years) with isolated TBI diagnosed on the basis of CT presentation of the head on admission were included in the study. The patients were divided into four groups: (i) severe brain injury (SHI) group (GCS ≤ 8), died within 2 weeks of injury (including near-death automatic discharge); (ii) moderate injury (MHI) (GCS > 8), survived injury and was discharged from hospital with a post-discharge follow-up GCS > 12, and the injuries were assessed using the GCS and computed tomography (CT) scan. CSF was collected intraoperatively (500 μl), and the samples were centrifuged at 3000 rpm for 10 min to remove cellular debris, and the supernatant was collected and stored at –80 °C until further analysis. PGK1 concentration was measured using enzyme-linked immunosorbent assay (ELISA) according to the manufacturer's instructions. GCS scores were obtained according to the Glasgow Coma Score (GCS) for cognitive function testing of the patients, and patients' prognosis was evaluated at discharge according to the GOS score.

Statistical Analysis

Data were expressed as mean ± standard deviation. Image J was applied for grayscale determination, SPSS 19.0 statistical software analysis. The experiments were replicated thrice under the same conditions, and the results were grayscaled and scanned for quantitative statistical analysis. Two-by-two comparison between groups was performed by using ANOVA. Linear correlation analysis was used to investigate the relationship between PGK1 and GCS and GOS scores. GCS scores were used to assess the severity of patients with TBI, and GOS scores were used to determine prognosis.

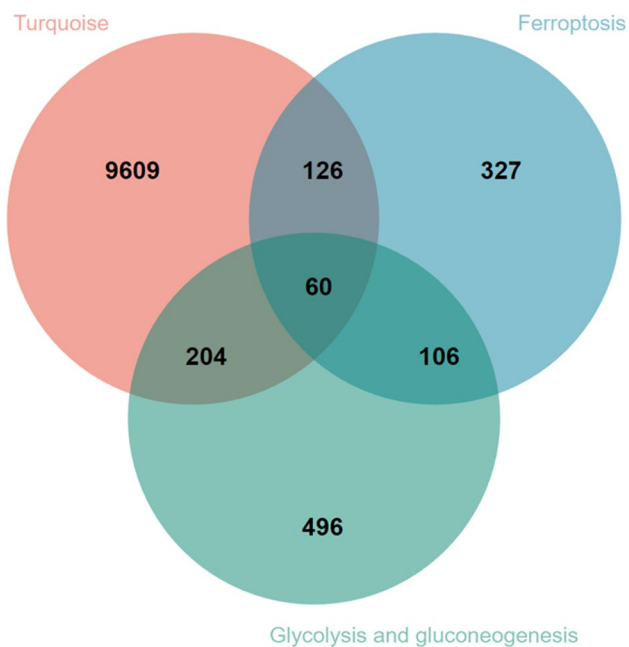


Fig. 2 Venn diagram: Yellow represents the turquoise module genes, and blue green represents ferroptosis genes. Green represents glycolysis and gluconeogenesis genes, and intersection represents dysregulated genes (DEGs)

Construction of TF–miRNA Interaction Networks and Prediction of PGK1 Targeting Drugs

We constructed a regulatory network to determine the regulatory mechanism of PGK1 gene with TF–miRNA (Fig. 5A). The results include 11 TFs, including HIF-1 α , STAT2, STAT1, SP1, PPARG, NFIL3, NFIC, MAX, GABPA, CTCF, and ATF1 and two miRNAs, including hsa-miR-143 and miR-873. We also predicted two drugs that could interfere with PGK1 activity (Fig. 5B), including the adenosine-5'-[beta, gamma-methylene] triphosphate and 3-phosphoglyceric acid.

TBI Model Mice Were Successfully Constructed

In this study, we evaluated the TBI mouse model and showed brain tissue injury, edema, and hematoma formation by HE staining. The hematoma was gradually absorbed over time (Fig. 6A). Thereafter, we assessed the neurological function of the TBI mice by using mNSS score, which showed that the neurological function of the mice was impaired after brain injury (Fig. 6B), and there was no significant difference between the injury groups. Finally, the brain water content (%) was calculated by the wet and dry method. The degree of brain edema indicated the degree of brain injury, and it was found that the brain edema was significantly severe in the 3-day TBI mice than in the sham group ($P < 0.05$);

however, there was no significant difference between other groups compared to the Sham group (Fig. 6C).

Validation of Hub Genes

We primarily verified the expressions of PGK1 and HIF-1 α involved in the HIF-1 signaling pathway in the TBI mice brain tissue. The WB results showed that the levels of PGK1 increased in the 3-h (1.363 ± 0.017), 1-day (1.867 ± 0.010), 3-day (1.867 ± 0.010), and 7-day (1.424 ± 0.006) TBI groups compared to the sham group; HIF-1 α levels increased in the 3-h (1.429 ± 0.008), 1-day (2.253 ± 0.016), 3-day (2.147 ± 0.080), and 7-day (1.858 ± 0.003) TBI samples, which peaked on day 1 and then decreased, but was elevated in all the groups compared to the sham group. The experiments were repeated thrice, and statistical analysis revealed significant differences (Fig. 7).

Immunofluorescence Verification of Hub Gene Localization After TBI

We selected the 1-day TBI group with the most obvious changes in hub gene expression for immunofluorescence staining. The immunofluorescence results showed that PGK1 was specifically expressed in neurons and microglia and primarily localized in cell cytoplasmic locations (Fig. 8A). In addition, upon labeling both HIF-1 α and PGK1, we found that they were co-localized in the same cells (Fig. 8B).

Levels of PGK1 Expression in CSF of TBI Patients

To assess the correlation between the CSF PGK1 levels and the severity of cranial injury, we examined 20 TBI patients with different prognosis, and classified the patients into SHI and MHI groups according to the GCS scores. No statistically significant differences were found when comparing general information between the two groups (Supplementary Table 2). The MHI group included eight cases, while the SHI group included 12 cases, with significant differences in the CSF PGK1 levels between the groups ($P < 0.001$). PGK1 expression level was higher in the MHI group than in the SHI group (Fig. 9A). Linear correlation analysis revealed a positive correlation between CSF PGK1 levels and GCS scores ($r = 0.7485$, $P < 0.01$) and a strong negative correlation between CSF PGK1 levels and GOS scores ($r = 0.7329$, $P < 0.01$) (Fig. 9B). Based on ROC curve analysis and calculation of AUC values, CSF PGK1 levels were all prognostic for TBI patients with an area under the curve (AUC) value of 0.8854 (Fig. 9C), and the level of CSF PGK1 ($\mu\text{g/mL}$) was relatively lower in patients with severe post-injury cranial injury at the time of admission than in MHI patients who survived until discharge. These results suggest that PGK1

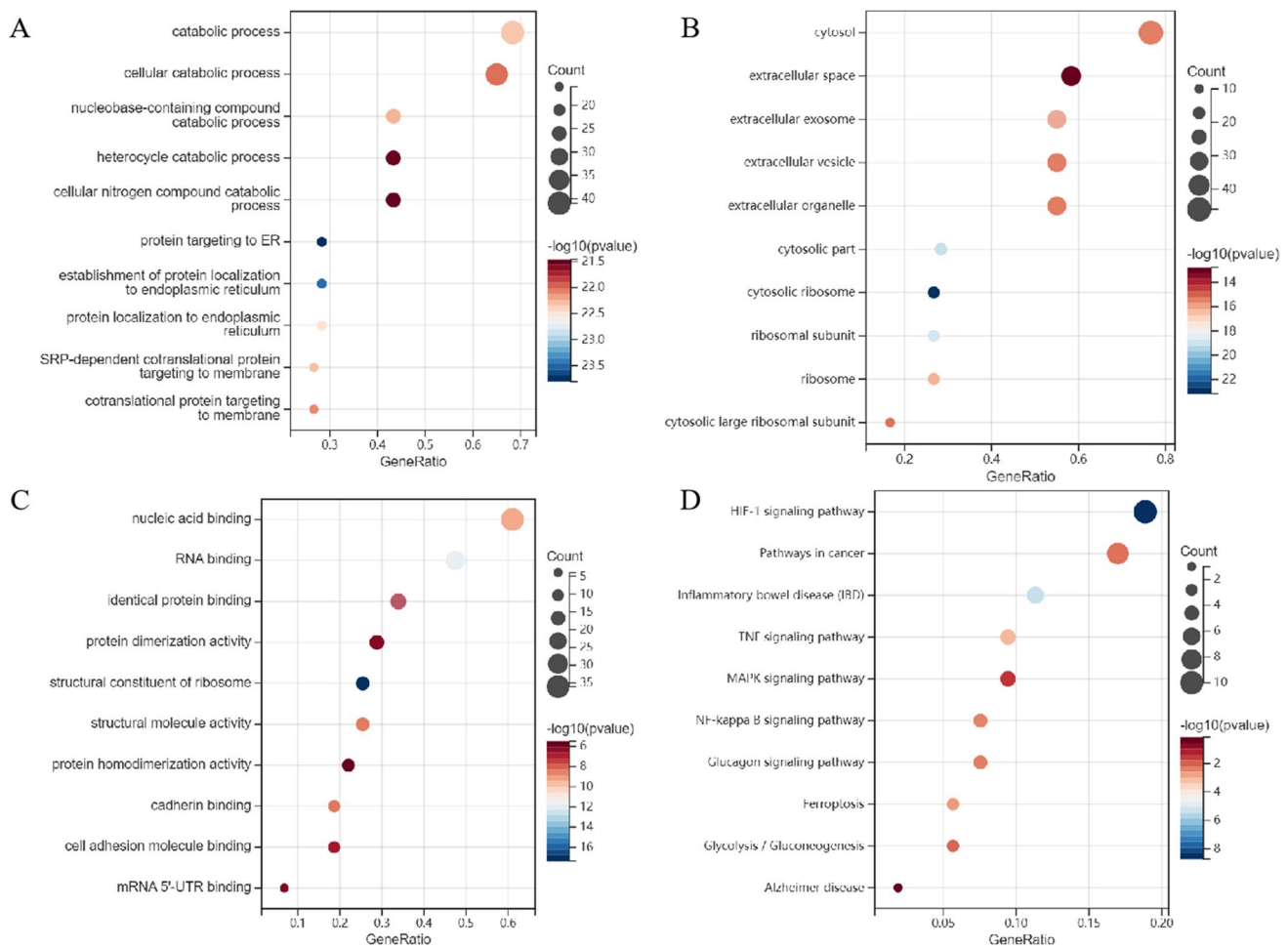


Fig. 3 Functional enrichment of the DEGs. **A** BP (biological process); **B** CC (cellular component); **C** MF (molecular function). **D** KEGG pathway enrichment analysis

Fig. 4 **A** Construction of PPI networks among the DEGs identified post-TBI. **B** Top 20 hub genes selected by Cyto-Hubba

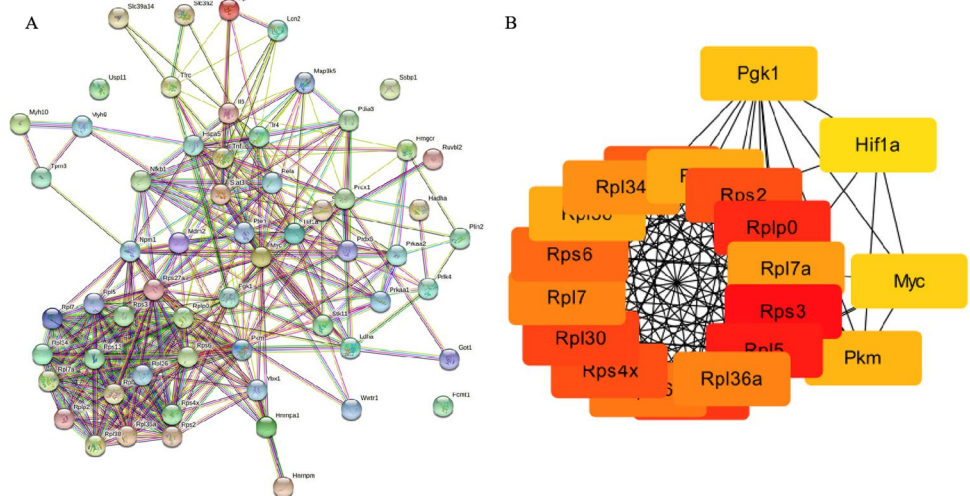


Fig. 5 **A** TF-miRNA regulatory network of central genes. Pink represents central genes, blue represents miRNAs, and green represents transcription factors; **B** predicted drugs for central genes. Pink represents central genes, and blue represents drugs

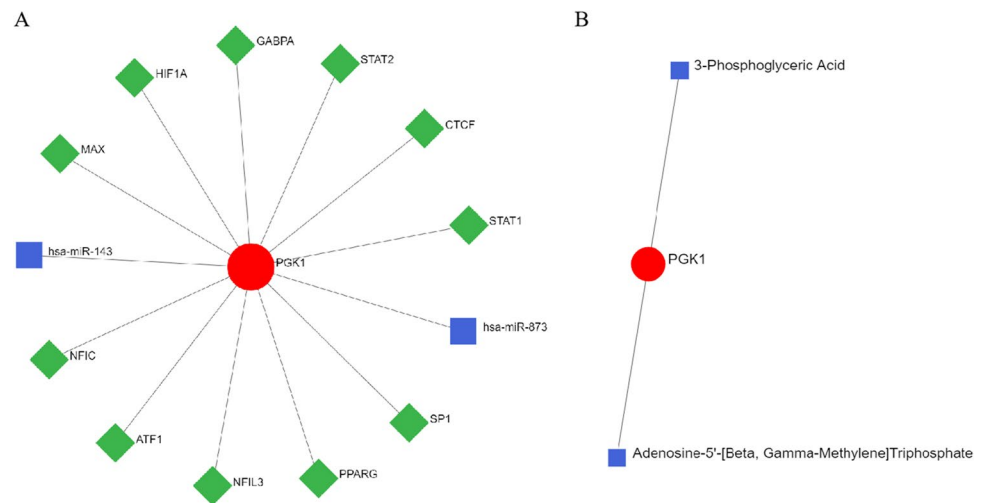
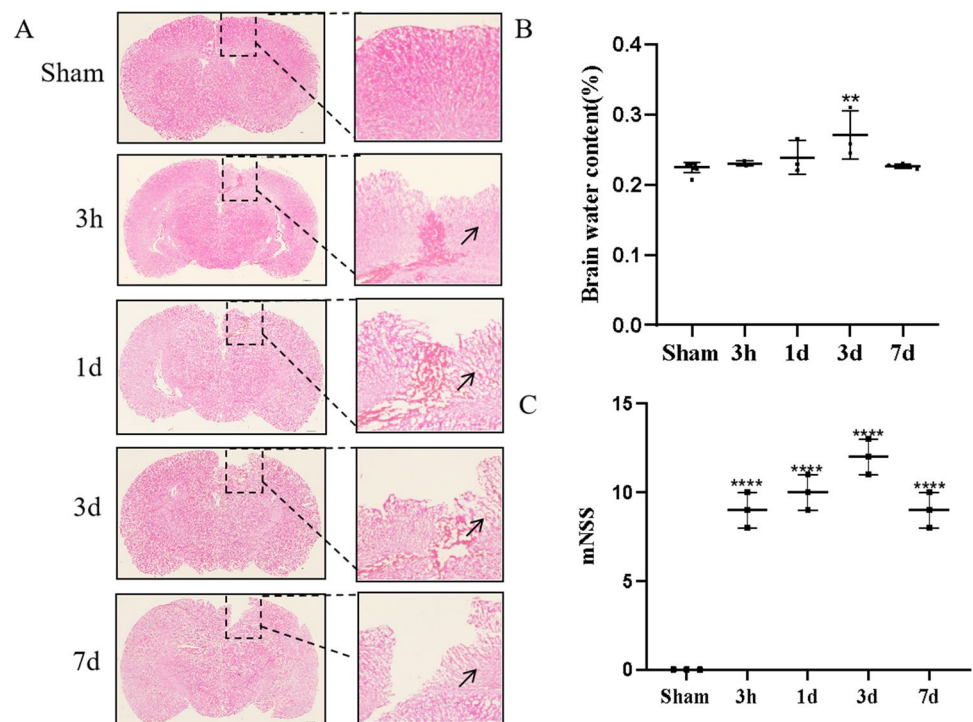


Fig. 6 **A** HE staining to detect significant tissue damage and hematoma formation and tissue edema after TBI (black arrow); **B** mNSS scores of mice were assessed before and 3 h, 1 day, 3 days, and 7 days after injury; **C** dry and wet method to detect brain edema. All experiments were repeated three times * $P < 0.05$, ** $P < 0.01$, *** $P < 0.001$, **** $P < 0.0001$



may improve patient prognosis, consistent with the predicted results.

Discussion

TBI is associated with high morbidity and mortality and imposes an enormous economic burden on individuals and societies worldwide. The pathophysiological process of TBI can be divided into two distinct stages: primary brain injury and secondary brain injury [27]. Primary brain injury is the main cause of patient prognosis, and subsequent secondary

brain injury can exacerbate the symptoms and worsen the prognosis of the TBI patients [28]. Ferroptosis is a newly discovered pattern of regulated cell death caused by iron-catalyzed lipid damage, which is significantly different from other known cell death pathways [29]. Ferroptosis is marked by iron-dependent reactive oxygen species (ROS) production, glutathione (GSH) level reduction, and glutathione peroxidase 4 (GPX4) inactivation [30, 31]. Many studies have found direct or indirect evidence for the involvement of ferroptosis in the pathological process of TBI. For instance, a study in mice found that iron accumulation and gene upregulation were associated with ferroptosis in mice experiencing

Fig. 7 Western blot detection of PGK1 and HIF1A expression in mouse brain tissue at different time points after TBI. All experiments were repeated three times * $P < 0.05$, ** $P < 0.01$, *** $P < 0.001$, **** $P < 0.0001$

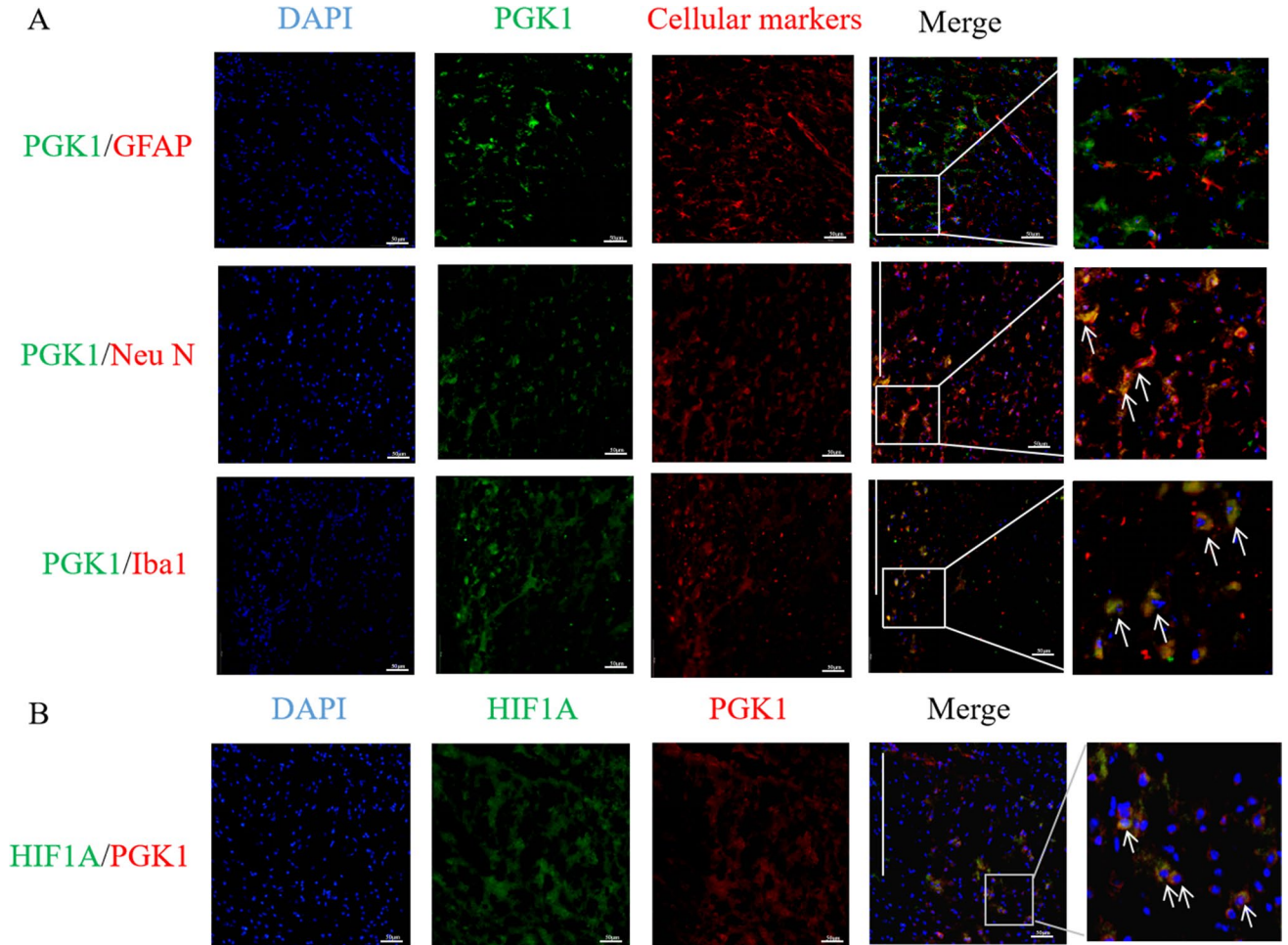
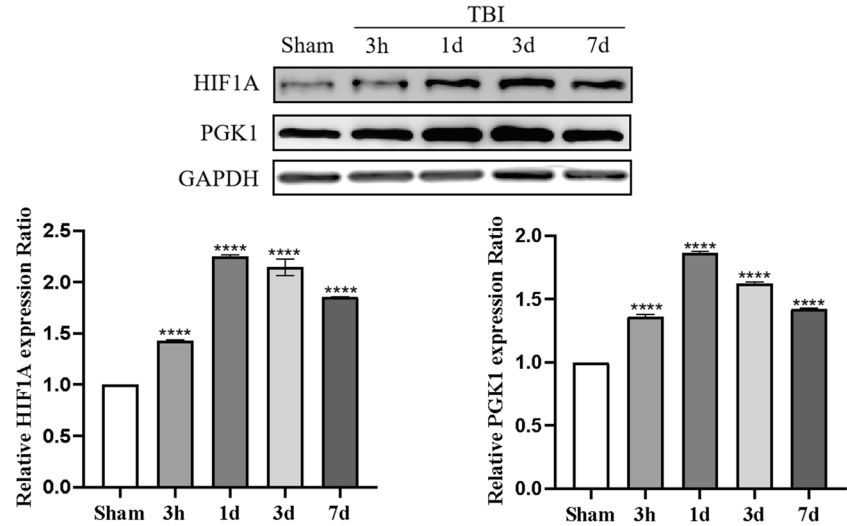
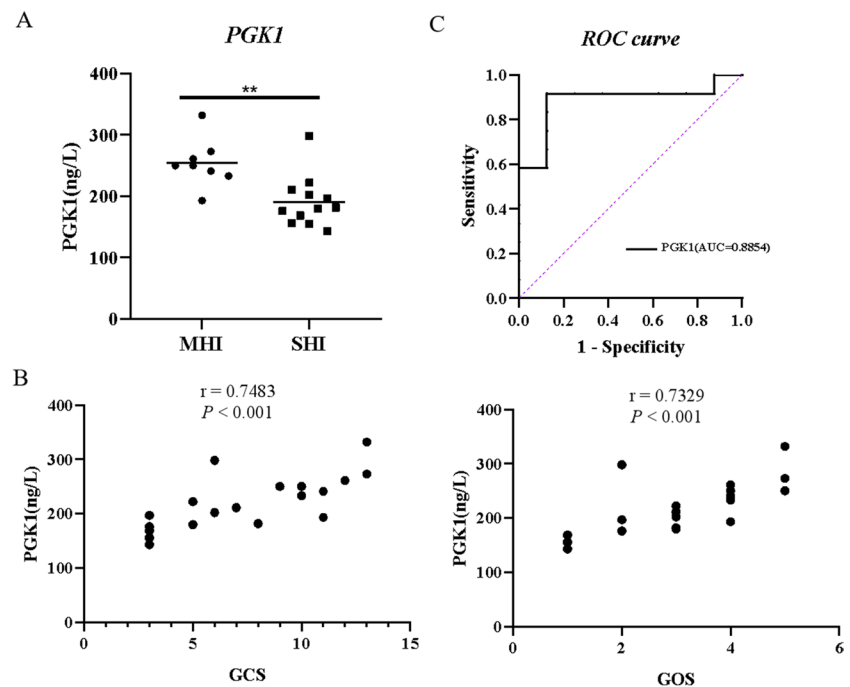


Fig. 8 **A** Immunostaining of GFAP (astrocytes), NeuN (neurons), Iba1 (microglia) (red), and PGK1 (green) around cortical injury in mice 1 day after cortical puncture injury. **B** Immunostaining of PGK1

(red) and HIF1A (green) around cortical injury in mice 1 day after cortical puncture injury, the white line shows the injury site, and cells are shown by arrows

Fig. 9 **A** Correlation of cerebrospinal fluid PGK1 levels in the two groups: moderate and mild head injury in MHI, severe head injury in SHI. Data are expressed as median (95–25th percentile). **B** Correlation analysis of CSF PGK1 levels with GCS and GOS scores. **C** ROC curves of CSF PGK1 in patients with TBI



TBI. Furthermore, ferroptosis inhibition ameliorates tissue damage and improves prognosis [32].

In this study, we used microarray data of ferroptosis-associated DEGs in mice, 48-h post-TBI and identified hub genes and hub pathways using various bioinformatics analyses. We obtained 60 DEGs from the crossover of GSE128543 dataset and ferroptosis and glycolytic/gluconeogenesis gene libraries. Thereafter, the DEGs were enriched using Metascape, GSEA, and DAVID, which revealed that these genes are primarily involved in HIF-1, TNF, MAPK, NF κ B, and ferroptosis signaling pathways. This study also screened several genes, such as *PGK1*, ribosomal protein (*RP*) family, *PKM*, *HIF-1 α* , and *MYC* associated with ferroptosis after TBI. We selected *PGK1* as the gene of interest and preliminarily explored the mechanism that may induce ferroptosis in TBI by activation of the HIF-1 pathway.

The HIF-1 signaling pathway is involved in the cellular response to hypoxia; high expression of HIF-1 facilitates neurological recovery in rats [33, 34]. The effect of HIF-1 on ferroptosis is achieved through the induction of transcription of fatty acid binding protein 3 and fatty acid binding protein 7 [26]. HIF-1 α can also be induced by the iron chelator desferrioxamine [35]. Additionally, a recent study showed that the HIF-1 signaling pathway plays an important role in the activation of the ferroptosis pathway after spinal cord injury [36]. The TNF signaling pathway plays an important role in inflammation and oxidative stress [37] and has immense research value. Additionally, previous experiments in mice showed that TNF- α treatment significantly increased glutamate levels, leading to astrocyte stress during neuroinflammation [38], which is considered to be an important target in

the pathophysiology of induced neurological damage [39]. Glutamate toxicity is closely associated with ferroptosis; therefore, TNF signaling pathways may play an important role post-TBI. Some signaling pathways, such as the MAPK pathway, are activated after oxidative stress. According to previous studies, MAPK and NF κ B pathways may induce the production of free radicals after cerebral hemorrhage, inducing ferroptosis and apoptosis. Therefore, antioxidant treatment may reduce ferroptosis as well as apoptosis in neurons after cerebral hemorrhage [40, 41]. Previous studies have confirmed that the MAPK pathway is activated following iron accumulation and that inhibition of MAPK activation improves functional outcomes and reduces neuronal cell death [42]. Thus, with the induction of ferroptosis, MAPK signaling pathway and NF κ B pathway may be activated to promote ROS generation, exacerbating cellular damage.

PGK1 catalyzes the transfer of phosphate between two intermediate products of carbohydrate metabolism [43]. In glycolysis, this enzyme catalyzes the transfer of the phosphate group from 1,3-BPGA to ADP to produce 3-phosphoglycerate and ATP, while it catalyzes the reverse reaction during glycoisomerization [20, 44]. The forward reaction is one of the two ATP-generating steps in the glycolytic pathway and is therefore important in the metabolism of many organisms. GAPDH/PGK interaction as a pH-dependent phenomenon has also been reported in human erythrocytes. This specific PPI between GAPDH and PGK may play a role in determining the fate of 1,3-BPGA produced in GAPDH-catalyzed reactions [45]. NADPH is an important intracellular reducing agent, and its abundance is a ferroptosis biomarker of sensitivity [46]. Recent studies have found that

ferroptosis suppressor protein 1 (FSP1) uses NADPH to regenerate coenzyme Q10 and inhibits ferroptosis of glutathione [47].

In the present study, we predicted the TF of *PGK1*, including HIF-1 α , which is significantly associated with ferroptosis. Subsequently, we constructed an in vivo mouse model of brain injury to further test this hypothesis. The results showed that *PGK1* plays an essential role in brain injury, especially as a novel ferroptosis activation mechanism post-TBI, which is mediated by activation of HIF-1 pathway. In this study, we demonstrated that *PGK1* expression upregulates HIF-1 α . Additionally, this study confirmed that *PGK1* may be involved in the HIF-1 pathway, which provides a direction for subsequent studies on the role of *PGK1* in ferroptosis post-TBI.

miRNAs are endogenous non-coding RNA molecules that target the 3'-UTR region of genes and regulate gene expression to degrade or inhibit translation of the target genes [48]. In our study, we predicted miRNAs, small molecule compounds, and drugs that may target and interfere with *PGK1* function. However, the role of these 11 TFs, 2 miRNAs, 2 drugs, and 79 small molecule compounds in ferroptosis has not been further validated, which is one of the limitations of this study. We performed in vivo experiments to create a TBI model, and WB analysis showed that HIF-1 α and *PGK1* were upregulated in the cerebral cortex of the TBI mice. Furthermore, immunofluorescence of cerebral cortical sections showed possible simultaneous null expression of both HIF-1 α and *PGK1*, and these results were consistent with the results of the previous studies and were re-validated by the analysis of the CSF of the TBI patients. Furthermore, in the present study, interventional experiments were not performed, and knockdown effect of *PGK1* gene on HIF-1 α and subsequent ferroptosis mechanism was not verified or elucidated, thus necessitating more in-depth studies. Additional limitations of this study are as follows: firstly, we only explored the DEGs associated with early brain injury post-TBI; therefore, the mechanisms of brain injury in the chronic phase post-TBI remain to be investigated. Secondly, this study also screened for DEGs other than *PGK1*, including RP family, PKM, and MYC, among which the RP family consists of many genes and could not be accommodated in this study, while the role of MYC in the ferroptosis process has already been elucidated in the previous studies. Thirdly, age, sex, body weight, and other characteristics of mice may be associated with the DEGs in TBI; however, we only explored the effects of TBI on mice of similar age, sex, and body weight. Lastly, we only studied DEGs in the cerebral cortex after TBI and other regions of the brain remain to be studied in future studies.

This study provides a comprehensive analysis of DEGs associated with TBI and further explores the relevance of *PGK1* associated with ferroptosis progression post-TBI.

Additionally, this study improves the ferroptosis-related database, as well as highlights the molecular mechanisms underlying the pathogenesis of secondary cortical injury post-TBI, based on the GEO database. Furthermore, it provides data supporting the existence of the *PGK1*–HIF-1 α ferroptosis pathway post-TBI; however, this study is a preliminary exploration and requires further studies to validate it. Therefore, the present study is only a preliminary investigation and requires further studies for validation of the predicted results.

Conclusion

In this study, we performed WGCNA of the GSE128543 dataset to identify the most relevant modules for TBI; we identified 60 DEGs by intersecting with ferroptosis and glycolysis/gluconeogenesis datasets. Among these, HIF-1, TNF, MAPK, and NF κ B were identified to be critical for ferroptosis post-TBI. The PPI network identified the top 20 hub genes, including *PGK1*, the RP family, PKM, HIF-1 α , and MYC genes. In this study, we selected *PGK1* as the gene of interest and explored the mechanism by which it may induce ferroptosis post-TBI via upregulation of HIF-1 α . Additionally, we established a mouse TBI model and WB analysis confirmed the upregulation of HIF-1 α and *PGK1* in the cerebral cortex of TBI mice. Moreover, immunofluorescence of the cerebral cortical sections showed the possible simultaneous null expression of both HIF-1 α and *PGK1*, consistent with the results of previous studies. Finally, we examined the expression of *PGK1* in the CSF of 20 clinical patients with different degrees of TBI within 48 h of surgery. The results showed that *PGK1* expression was detected differently in the CSF of patients with different degrees of TBI, and its expression level was negatively correlated with the severity of the TBI, which suggested that *PGK1* may be a potential hub gene for ferroptosis, second to neurological injury, post-TBI, affecting patient prognosis. In conclusion, this study contributes to the understanding of ferroptosis induced by TBI and provides new insights into the clinical treatment strategy for TBI.

Supplementary Information The online version contains supplementary material available at <https://doi.org/10.1007/s12035-024-04170-z>.

Acknowledgements We appreciate Dr. Chengwei Duan (Center for Scientific Research of The Second Affiliated Hospital of Nantong University) for his guidance.

Author Contribution All authors contributed to the study conception and design. Yi Zhang, Sujuan Feng, and Hongyan Yan designed the study. Zhao Wang and Jinjie Tian performed the animal experiments and bioinformatic analysis together with the help of Yi Zhang and Lei Wang. Zhao Wang performed HE stain and immunofluorescence assay. Jinjie Tian performed the WB test. Zhao Wang and Jinjie Tian analysis of cerebrospinal fluid and prognosis in patients with TBI. Zhao Wang and Jinjie Tian performed ELISA assay. Zhao Wang, Yi Zhang, and

Jinjie Tian wrote the manuscript. All authors reviewed and concurred with the final manuscript. Zhao Wang and Yi Zhang took responsibility for the whole study. All authors read and approved the final manuscript.

Funding This study was supported by the Science and Technology Support Program of Nantong (JC2021179), Scientific Research Foundation of Nantong Health Committee (MB2021026), “Scientific research innovation team project” of Kangda College of Nanjing Medical University (KD2022KYCXTD006) and “Top Six Types of Talents” Financial Assistance of Jiangsu Province Grant (WSW-199), the General Program of Traditional Chinese Medicine Administration of Jiangsu Provincial Health Commission (MS2021060).

Data Availability The datasets analyzed during the current study are available in the Gene Expression Omnibus (GEO) database repository, GEO Accession viewer (nih.gov). The original contributions presented in the study are included in the article/supplementary material. Further inquiries can be directed to the corresponding authors.

Declarations

Ethics Approval and Consent to Participate The study protocols regarding the animals were approved by the Ethics Committee of Nantong University of China (No.S20220221-048).

Conflict of Interest The authors declare no competing interests.

References

- Joseph B, Haider A, Rhee P (2015) Traumatic brain injury advancements. *Curr Opin Crit Care* 21(6):506–511. <https://doi.org/10.1097/MCC.0000000000000247>
- Königs M, Engenhorst PJ, Oosterlaan J (2016) Intelligence after traumatic brain injury: meta-analysis of outcomes and prognosis. *Eur J Neurol* 23(1):21–29. <https://doi.org/10.1111/ene.12719>
- Bramlett HM, Dietrich WD (2015) Long-term consequences of traumatic brain injury: current status of potential mechanisms of injury and neurological outcomes. *J Neurotrauma* 32(23):1834–1848. <https://doi.org/10.1089/neu.2014.3352>
- Johansson B, Andréll P, Rönnbäck L, Mannheimer C (2020) Follow-up after 55 years of treatment with methylphenidate for mental fatigue and cognitive function after a mild traumatic brain injury. *Brain Inj* 34(2):229–235. <https://doi.org/10.1080/02699052.2019.1683898>
- Yang X, Chen Y, Li J, Chen L, Ren H, Liu Y, Zhang X (2019) Hypertonic saline maintains coagulofibrinolytic homeostasis following moderate-to-severe traumatic brain injury by regulating monocyte phenotype via expression of lncRNAs. *Mol Med Rep* 19(2):1083–1091. <https://doi.org/10.3892/mmr.2018.9748>
- Timofeev I, Nortje J, Al-Rawi PG, Hutchinson PJ, Gupta AK (2013) Extracellular brain pH with or without hypoxia is a marker of profound metabolic derangement and increased mortality after traumatic brain injury. *J Cereb Blood Flow Metab* 33(3):422–427. <https://doi.org/10.1038/jcbfm.2012.186>
- Carteron L, Bouzat P, Oddo M (2017) Cerebral microdialysis monitoring to improve individualized neurointensive care therapy: an update of recent clinical data. *Front Neurol* 8:281870. <https://doi.org/10.3389/fneur.2017.00601>
- Timofeev I, Carpenter KL, Nortje J, Al-Rawi PG, O’Connell MT, Czosnyka M, Smielewski P, Pickard JD et al (2011) Cerebral extracellular chemistry and outcome following traumatic brain injury: a microdialysis study of 223 patients. *Brain* 134(Pt 2):484–494. <https://doi.org/10.1093/brain/awq353>
- Dixon SJ, Lemberg KM, Lamprecht MR, Skouta R, Zaitsev EM, Gleason CE, Patel DN, Bauer AJ et al (2012) Ferroptosis: an iron-dependent form of nonapoptotic cell death. *Cell* 149(5):1060–1072. <https://doi.org/10.1016/j.cell.2012.03.042>
- Yang WS, SriRamaratnam R, Welsch ME, Shimada K, Skouta R, Viswanathan VS, Cheah JH, Clemens PA et al (2014) Regulation of ferroptotic cancer cell death by GPX4. *Cell* 156(1–2):317–331. <https://doi.org/10.1016/j.cell.2013.12.010>
- Zille M, Karuppagounder SS, Chen Y, Gough PJ, Bertin J, Finger J, Milner TA, Jonas EA et al (2017) Neuronal death after hemorrhagic stroke in vitro and in vivo shares features of ferroptosis and necroptosis. *Stroke* 48(4):1033–1043. <https://doi.org/10.1161/STROKEAHA.116.015609>
- Li Y, Cao Y, Xiao J, Shang J, Tan Q, Ping F, Huang W, Wu F et al (2020) Inhibitor of apoptosis-stimulating protein of p53 inhibits ferroptosis and alleviates intestinal ischemia/reperfusion-induced acute lung injury. *Cell Death Differ* 27(9):2635–2650. <https://doi.org/10.1038/s41418-020-0528-x>
- Friedmann Angeli JP, Schneider M, Proneth B, Tyurina YY, Tyurin VA, Hammond VJ, Herbach N, Aichler M et al (2014) Inactivation of the ferroptosis regulator Gpx4 triggers acute renal failure in mice. *Nat Cell Biol* 16(12):1180–1191. <https://doi.org/10.1038/ncb3064>
- Bao WD, Pang P, Zhou XT, Hu F, Xiong W, Chen K, Wang J, Wang F et al (2021) Loss of ferroportin induces memory impairment by promoting ferroptosis in Alzheimer’s disease. *Cell Death Differ* 28(5):1548–1562. <https://doi.org/10.1038/s41418-020-00685-9>
- Yusuf RZ, Saez B, Sharda A, van Gestel N, Yu V, Baryawno N, Scadden EW, Acharya S et al (2020) Aldehyde dehydrogenase 3a2 protects AML cells from oxidative death and the synthetic lethality of ferroptosis inducers. *Blood* 136(11):1303–1316. <https://doi.org/10.1182/blood.2019.001808>
- Kenny EM, Fidan E, Yang Q, Anthonyamuthu TS, New LA, Meyer EA, Wang H, Kochanek PM et al (2019) Ferroptosis contributes to neuronal death and functional outcome after traumatic brain injury. *Crit Care Med* 47(3):410–418. <https://doi.org/10.1097/CCM.0000000000003555>
- Eleftheriadis T, Pissas G, Filippidis G, Liakopoulos V, Stefanidis I (2021) Reoxygenation induces reactive oxygen species production and ferroptosis in renal tubular epithelial cells by activating aryl hydrocarbon receptor. *Mol Med Rep* 23(1):41. <https://doi.org/10.3892/mmr.2020.1679>
- Yuan S, Wei C, Liu G, Zhang L, Li J, Li L, Cai S, Fang L (2022) Sorafenib attenuates liver fibrosis by triggering hepatic stellate cell ferroptosis via HIF-1 α /SLC7A11 pathway. *Cell proliferation* 55(1):e13158. <https://doi.org/10.1111/cpr.13158>
- Jha RM, Kochanek PM, Simard JM (2019) Pathophysiology and treatment of cerebral edema in traumatic brain injury. *Neuropharmacol* 145(Pt B):230–246. <https://doi.org/10.1016/j.neuropharm.2018.08.004>
- Banks RD, Blake CC, Evans PR, Haser R, Rice DW, Hardy GW, Merrett M, Phillips AW (1979) Sequence, structure and activity of phosphoglycerate kinase: a possible hinge-bending enzyme. *Nature* 279(5716):773–777. <https://doi.org/10.1038/279773a0>
- Ye T, Liang Y, Zhang D, Zhang X (2020) MicroRNA-16-1-3p represses breast tumor growth and metastasis by inhibiting PKG1-mediated Warburg effect. *Front Cell Dev Biol* 8:615154. <https://doi.org/10.3389/fcell.2020.061514>
- Amorini AM, Lazzarino G, Di Pietro V, Signoretti S, Lazzarino G, Belli A, Tavazzi B (2016) Metabolic, enzymatic and gene involvement in cerebral glucose dysmetabolism after traumatic brain injury. *Biochimica et biophysica acta* 1862(4):679–687. <https://doi.org/10.1016/j.bbadis.2016.01.023>
- Grandjean G, Jong PR, James B, Koh MY, Lemos R, Kingston J, Aleshin A, Bankston LA et al (2016) Definition of a novel

- feed-forward mechanism for glycolysis-HIF1 α signaling in hypoxic tumors highlights aldolase A as a therapeutic target. *Cancer Res* 76(14):4259–4269. <https://doi.org/10.1158/0008-5472.CAN-16-0401>
24. Fu D, He C, Wei J, Zhang Z, Luo Y, Tan H, Ren C (2018) PGK1 is a potential survival biomarker and invasion promoter by regulating the HIF-1 α -mediated epithelial-mesenchymal transition process in breast cancer. *Cell Physiol Biochem* 51(5):2434–2444. <https://doi.org/10.1159/000495900>
 25. Yuan D, Guan S, Wang Z, Ni H, Ding D, Xu W, Li G (2021) HIF-1 α aggravated traumatic brain injury by NLRP3 inflammasome-mediated pyroptosis and activation of microglia. *J Chem Neuroanat* 116:101994. <https://doi.org/10.1016/j.jchemneu.2021.101994>
 26. Yang M, Chen P, Liu J, Zhu S, Kroemer G, Klionsky DJ, Lotze MT, Zeh HJ et al (2019) Clockophagy is a novel selective autophagy process favoring ferroptosis. *Sci Adv* 5(7):eaaw2238. <https://doi.org/10.1126/sciadv.aaw2238>
 27. Hawryluk G, Rubiano AM, Totten AM, O'Reilly C, Ullman JS, Bratton SL, Chesnut R, Harris OA et al (2020) Guidelines for the management of severe traumatic brain injury: 2020 update of the decompressive craniectomy recommendations. *Neurosurgery* 87(3):427–434. <https://doi.org/10.1093/neuros/nyaa278>
 28. Shi H, Hua X, Kong D, Stein D, Hua F (2019) Role of Toll-like receptor mediated signaling in traumatic brain injury. *Neuropharmacology* 145(Pt B):259–267. <https://doi.org/10.1016/j.neuropharm.2018.07.022>
 29. Stockwell BR, Friedmann Angeli JP, Bayir H, Bush AI, Conrad M, Dixon SJ, Fulda S, Gascón S et al (2017) Ferroptosis: a regulated cell death nexus linking metabolism, redox biology, and disease. *Cell* 171(2):273–285. <https://doi.org/10.1016/j.cell.2017.09.021>
 30. Hirschhorn T, Stockwell BR (2019) The development of the concept of ferroptosis. *Free Radic Biol Med* 133:130–143. <https://doi.org/10.1016/j.freeradbiomed.2018.09.043>
 31. Su LJ, Zhang JH, Gomez H, Murugan R, Hong X, Xu D, Jiang F, Peng ZY (2019) Reactive oxygen species-induced lipid peroxidation in apoptosis, autophagy, and ferroptosis. *Oxidative medicine and cellular longevity* 2019:5080843. <https://doi.org/10.1155/2019/5080843>
 32. Xie BS, Wang YQ, Lin Y, Mao Q, Feng JF, Gao GY, Jiang JY (2019) Inhibition of ferroptosis attenuates tissue damage and improves long-term outcomes after traumatic brain injury in mice. *CNS Neurosci Ther* 25(4):465–475. <https://doi.org/10.1111/cns.13069>
 33. Han X, Chen Y, Liu Y, Wang Z, Tang G, Tian W (2018) HIF-1 α promotes bone marrow stromal cell migration to the injury site and enhances functional recovery after spinal cord injury in rats. *J Gene Med* 20(12):e3062. <https://doi.org/10.1002/jgm.3062>
 34. Luo Z, Wu F, Xue E, Huang L, Yan P, Pan X, Zhou Y (2019) Hypoxia preconditioning promotes bone marrow mesenchymal stem cells survival by inducing HIF-1 α in injured neuronal cells derived exosomes culture system. *Cell death disease* 10(2):134. <https://doi.org/10.1038/s41419-019-1410-y>
 35. Woo KJ, Lee TJ, Park JW, Kwon TK (2006) Desferrioxamine, an iron chelator, enhances HIF-1 α accumulation via cyclooxygenase-2 signaling pathway. *Biochem Biophys Res Commun* 343(1):8–14. <https://doi.org/10.1016/j.bbrc.2006.02.116>
 36. Kang Y, Li Q, Zhu R, Li S, Xu X, Shi X, Yin Z (2022) Identification of ferroptotic genes in spinal cord injury at different time points: bioinformatics and experimental validation. *Mol Neurobiol* 59(9):5766–5784. <https://doi.org/10.1007/s12035-022-02935-y>
 37. Fischer R, Maier O (2015) Interrelation of oxidative stress and inflammation in neurodegenerative disease: role of TNF. *Oxid Med Cell Longev* 2015:610813. <https://doi.org/10.1155/2015/610813>
 38. Wang K, Ye L, Lu H, Chen H, Zhang Y, Huang Y, Zheng JC (2017) TNF- α promotes extracellular vesicle release in mouse astrocytes through glutaminase. *J Neuroinflammation* 14(1):87. <https://doi.org/10.1186/s12974-017-0853-2>
 39. Shah SA, Amin FU, Khan M, Abid MN, Rehman SU, Kim TH, Kim MW, Kim MO (2016) Anthocyanins abrogate glutamate-induced AMPK activation, oxidative stress, neuroinflammation, and neurodegeneration in postnatal rat brain. *J Neuroinflammation* 13(1):286. <https://doi.org/10.1186/s12974-016-0752-y>
 40. Haddad JJ, Land SC (2002) Redox/ROS regulation of lipopolysaccharide-induced mitogen-activated protein kinase (MAPK) activation and MAPK-mediated TNF- α biosynthesis. *Br J Pharmacol* 135(2):520–536. <https://doi.org/10.1038/sbjbp0704467>
 41. Speer RE, Karuppagounder SS, Basso M, Sleiman SF, Kumar A, Brand D, Smirnova N, Gazaryan I et al (2013) Hypoxia-inducible factor prolyl hydroxylases as targets for neuroprotection by “antioxidant” metal chelators: from ferroptosis to stroke. *Free Radic Biol Med* 62:26–36. <https://doi.org/10.1016/j.freeradbiomed.2013.01.026>
 42. Yu Y, Richardson DR (2011) Cellular iron depletion stimulates the JNK and p38 MAPK signaling transduction pathways, dissociation of ASK1-thioredoxin, and activation of ASK1. *J Biol Chem* 286(17):15413–15427. <https://doi.org/10.1074/jbc.M111225946>
 43. Palmaí Z, Seifert C, Gräter F, Balog E (2014) An allosteric signaling pathway of human 3-phosphoglycerate kinase from force distribution analysis. *PLoS Comput Biol* 10(1):e1003444. <https://doi.org/10.1371/journal.pcbi.1003444>
 44. VanItallie TB (2019) Traumatic brain injury (TBI) in collision sports: possible mechanisms of transformation into chronic traumatic encephalopathy (CTE). *Metabolism* 100S:153943. <https://doi.org/10.1016/j.jmetabol.2019.07.007>
 45. Fokina KV, Dainyak MB, Nagradova NK, Muronetz VI (1997) A study on the complexes between human erythrocyte enzymes participating in the conversions of 1,3-diphosphoglycerate. *Arch Biochem Biophys* 345(2):185–192. <https://doi.org/10.1006/abbi.1997.0222>
 46. Shimada K, Hayano M, Pagano NC, Stockwell BR (2016) Cell-line selectivity improves the predictive power of pharmacogenomic analyses and helps identify NADPH as biomarker for ferroptosis sensitivity. *Cell Chem Biol* 23(2):225–235. <https://doi.org/10.1016/j.jchembiol.2015.11.016>
 47. Doll S, Freitas FP, Shah R, Aldrovandi M, Silva MC, Ingold I, Goya Grocin A, Xavier da Silva TN et al (2019) FSP1 is a glutathione-independent ferroptosis suppressor. *Nature* 575(7784):693–698. <https://doi.org/10.1038/s41586-019-1707-0>
 48. Sun KT, Chen MY, Tu MG, Wang IK, Chang SS, Li CY (2015) MicroRNA-20a regulates autophagy related protein-ATG16L1 in hypoxia-induced osteoclast differentiation. *Bone* 73:145–153. <https://doi.org/10.1016/j.bone.2014.11.026>

Publisher's Note Springer Nature remains neutral with regard to jurisdictional claims in published maps and institutional affiliations.

Springer Nature or its licensor (e.g. a society or other partner) holds exclusive rights to this article under a publishing agreement with the author(s) or other rightsholder(s); author self-archiving of the accepted manuscript version of this article is solely governed by the terms of such publishing agreement and applicable law.